# Thermal Design of a Cabinet With Heat Sinks Using CFD Analysis

**Heng Ren**

*Abstract*— **Power device cooling has an important effect on the performance and dependability of the whole electronic equipment. In this paper, the thermal simulation of an airtight cabinet is carried out by means of the CFD software Icepak. The flow and temperature fields of the heat sink are investigated as a conjugate heat transfer problem. The simulation results show that the cooling method of forced convection can control the final temperature of the main power device below 85 degree, which is acceptable in view of stable working. Moreover, the effects of materials and base thicknesses of the heat sink are analyzed. It is found that replacing aluminum with copper as the heat sink material can improve the cooling effect, and the heat sink with thicker base has lower temperatures.**

*Index Terms*— **Cabinet, heat sink, forced convection, Icepak.**

## [1] INTRODUCTION

Electronic equipment should operate within a limited temperature range for acceptable reliability. Aa a designer, accurate prediction of the equipment operating temperature is necessary at the earliest possible stages of design. Due to the high power dissipation values of the devices, it results in localized hot spots around the devices. These hot spots will cause high junction temperature of the devices [1]. Generally speaking, the higher the junction temperature is, the lower the reliability will be. Thus, the thermal management of electronic devices is very important. Among all the available cooling methods, forced convection air cooling is the most common approach. In this direct heat removal approach, a fan is installed to a heat sink forming an assembly. Air is forced through the heat sink by the fan; thus, the heat is directly transferred to the final heat transfer medium - air.

Simulation software is a good tool to reduce design cycles and prototypes. Compared with the experimental measurement, simulation can be beneficial in several ways: low cost (generally cheaper than experimental study), speed (generally quick implications of many configurations can be studied in a short time), optimization, complete information (detailed information, e.g. velocity, pressure, temperature etc.), and quickly simulate realistic conditions (high temperature, high altitude, zero gravity). Computational fluid dynamic (CFD) simulations have not entered electronics cooling area for a long time. Before the last decade, it was very expensive to perform CFD calculations, but with the introduction of high power workstations and personal computers, the cost of such computations has been drastically reduced. CFD software can help to analyze and predict all aspects of thermal problems in electronic cooling.

Several researchers have worked on conjugate heat transfer in electronic systems via CFD. Yu and Webb [2] simulated a complete desktop computer system. They solved the whole domain with a commercial software package Icepak. Biswas et al. [3] also used Icepak to study the airflow in a compact electronic enclosure. Their investigated the pressure loss due to the presence of the inlet and the outlet grilles. Linton and Agonafer [4] compared the results of a detailed CFD modeling of a heat sink with experimental data. They found that the coarse model agrees well with the detailed model without losing the characteristics of the heat sink. Sathyamurthy and Runstadler [5] studied planar and staggered heat sink performance with Fluent. They found that the thermal performance of staggered fin configuration is superior over planar fin configuration. Yu et al. [6] combined pin fins with plane fins to obtain a heat sink design called plate-pin fin heat sink. Eveloy et al. [7] used Flotherm as a design tool to predict component temperature on printed circuit boards. Bar-Cohen and his coworkers [8-9] investigated the cooling effect of forced convection heat sinks with various plane fin or pin fin geometries.

In this paper, CFD is utilized to investigate the fluid flow and heat transfer in an airtight cabinet. Fluent is used to solve the Navier-Stokes equations, while Icepak is used for pre-processing and post-processing. Detailed modeling of the whole cabinet together with the densely meshed heat sink (about 50% of the cells are used for the heat sink) is selected over the so called zoom-in modeling that is commonly used for modeling interesting parts of the domain in detail.

## [2] GOVERNING EQUATIONS

Time-independent flow equations with turbulence are solved. The viscous dissipation term is omitted. Therefore, the governing equations for the fluid flow are the following form of the incompressible equations, including continuity, *x*-, *y*-, and *z*-direction momentum, and energy equations. In the equations, ($u$, $v$, $w$) are the components of the fluid velocity $\vec{V}$ in ($x$, $y$, $z$) directions; $\rho$ is the density; $p$ is the pressure; $T$ is the temperature, $h_0$ is the total enthalpy, and $R$ is the ideal gas constant; $S$ and $\tau$ are the directional body force and shear stresses. In the energy equation (5), the effective thermal conductivity is defined as $k_{\text{eff}} = k + k_t$, where $k_t$ is the turbulent conductivity term.

***Manuscript received June 24, 2015.***

***Heng Ren**, China Electronics Technology Group Corporation No.38 Research Institute, Hefei, China, +86 18900518514.*



ISSN: 2278 – 7798 

$$\nabla\cdot\left(\rho\vec{V}\right)=0 \quad (1)$$

$$\nabla\cdot\left(\rho u\vec{V}\right)=-\frac{\partial p}{\partial x}+\frac{\partial \tau_{xx}}{\partial x}+\frac{\partial \tau_{yx}}{\partial y}+\frac{\partial \tau_{zx}}{\partial z}+S_{Mx} \quad (2)$$

$$\nabla\cdot\left(\rho v\vec{V}\right)=-\frac{\partial p}{\partial y}+\frac{\partial \tau_{xy}}{\partial x}+\frac{\partial \tau_{yy}}{\partial y}+\frac{\partial \tau_{zy}}{\partial z}+S_{Mx} \quad (3)$$

$$\nabla\cdot\left(\rho w\vec{V}\right)=-\frac{\partial p}{\partial z}+\frac{\partial \tau_{xz}}{\partial x}+\frac{\partial \tau_{yz}}{\partial y}+\frac{\partial \tau_{zz}}{\partial z}+S_{Mz} \quad (4)$$

$$\nabla\cdot\left(\rho h_0\vec{V}\right)=-p\nabla\cdot\vec{V}+\nabla\cdot\left(k_{eff}\nabla T\right)+S_h \quad (5)$$

$$p=\rho RT \quad (6)$$

The Reynolds averaging is employed to handle the turbulence effects. In the Reynolds averaging, the solution variables are decomposed into mean and fluctuating components. For the velocity, $u=\bar{u}+u'$, where $\bar{u}$ and $u'$ are the mean and fluctuating velocity components for *x*-direction. Likewise, for the pressure and the other scalar quantities $\phi=\bar{\phi}+\phi'$, where $\phi$ is a scalar such as pressure or energy. The Reynolds Averaged Navier-Stokes (RANS) equations are solved together with the Boussinesq approximation.

## [3] Computation Model and Boundary Conditions

### A. *Computational model*

The whole airtight cabinet is the computational domain, as shown in Fig. 1. It is a 3-D model of a common cabinet in dimensions of $L \times W \times H = 450$ mm $\times$ 400 mm $\times$ 180 mm. Since the aim of this study is the investigation of temperature distributions on heat sink, the other power devices will not introduce in detail. The model of the aluminum heat sink is shown in Fig. 2. The total size is $L \times W \times H = 90$ mm $\times$ 90 mm $\times$ 52 mm. The aluminum pins are 52 mm high, 2.5 mm $\times$ 2.5 mm in size, and spaced 2 mm apart. The base of the heat sink is composed of aluminum and a large copper, and the thickness is 9 mm. The copper base inserts 4 mm thick, by 72 mm $\times$ 62 mm in size. A 20 mm $\times$ 20 mm square heat source with 80 W heat dissipation rate locates on the center of the base plate. Moreover, at each corner of the heat sink, a small amount of the base has been milled away so that there is sufficient space between the heat sink and the brass stand offs which need to be installed on the printed board.

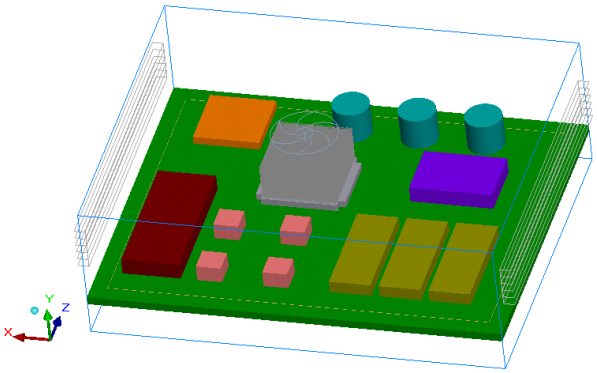

Fig. 1. Computational domain.

The fan draws air in through the pins in the heat sink, before exhausting it into the cabinet. In the domain, the fan is modeled as a zero thickness pressure jump, which adds momentum source to the flow. The point where the fan is going to operate is calculated iteratively from the system pressure curve. The relationship between the pressure and the flow rate is assumed to be linear. In the computation, the ambient air temperature is specified at 45 °C.

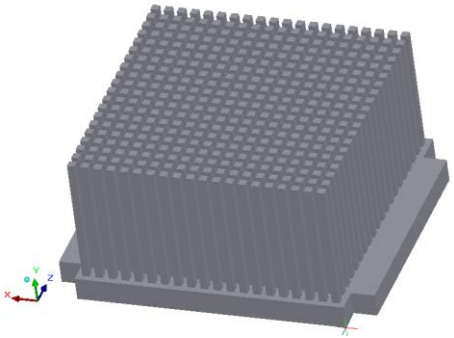

Fig. 2. Model of heat sink.

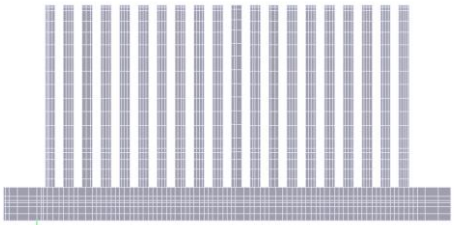

Fig. 3. The unstructured mesh of heat sink in *x-y* plane.

The mesh is unstructured, and the density distribution of the mesh is concentrated around the heat sink. In the present study, the total elements of the cabinet are approximately 1300,000, and 648857 cells are in the non-conformal mesh of the heat sink. A closer meshed view of the heat sink generated by Icepak is shown in Fig. 3. Conjugate conduction and convection heat transfer inside the cabinet is solved using finite volume method.

### B. *Boundary conditions*

In the computation, the Navier – Stokes equations are solved inside the computational domain, and no-slip boundary condition is applied to all the walls in the domain.

It is assumed that the heat transfer mechanism at the cabinet outer walls is natural convection. Heat transfer coefficients at the outer walls can be estimated from the empirical correlations. After the heat transfer coefficients are calculated, they are applied to all of the exterior walls of the cabinet except the bottom horizontal wall which sits on the ground that is considered to be adiabatic.

Öztürk investigated the radiation effects on heat sink [10]. They found that the radiation heat transfer helped the heat sink cool by less than additional 0.5 °C. Therefore, the radiation can be ignored for forced cooling in present study.

### C. *Thermal Resistance*

Based on the 80W power chip thermal specification, 85 °C copper base plate temperature limit, and 45 °C ambient temperature, the required total thermal resistance for the heat sink is:



ISSN: 2278 – 7798 

$$R_{tot} = \frac{T_c - T_a}{\dot{q}} = 0.5\,°C/W, \quad (7)$$

where $T_c$ is the copper base plate temperature, and $T_a$ is the ambient air temperature.

The $T_{tot}$ represents the sum of three thermal resistances, which is given by

$$R_{tot} = R_{\text{int}} + R_{sp} + R_{cv}, \quad (8)$$

where $R_{int}$ is the chip-to-heat sink interface resistance, $R_{sp}$ is the spreading resistance in the heat sink base plate, and $R_{cv}$ is the convection thermal resistance of the heat sink. The total heat sink resistance is equal to $R_{sp} + R_{cv}$.

In the present study, $R_{sp}$ is chosen as 0.08 °C/W, which is nearly independent of the air velocity under consideration. The thermal resistance $R_{int}$ for the thermal grease interface material is 0.18 °C /W based on the 20 mm × 20 mm contact area.

## [4] RESULTS AND DISCUSSION

### *A. Temperature and Air Flow Pattern Distributions*

The temperature distributions for the whole cabinet are shown in Fig. 4. It is seen that the maximum temperature is 84.4 °C. Figures 5 and 6 show the temperature distribution of the heat sink, the maximum temperature is 78.9 °C. It can be stated that some hot spots locate on the center of the heat sink, since the heat source corresponds to the proximity of the base center. The fan installed on the heat sinks is identical with dimensions and fan curves. The fan has a hub where air cannot pass through and it makes the center parts hotter, as shown in Fig. 6. In the current simulation, the swirl of the fan is not modeled since the fan is lumped parameter models. For real case, the center would not be as hot as the present simulation predict, due to the swirl.

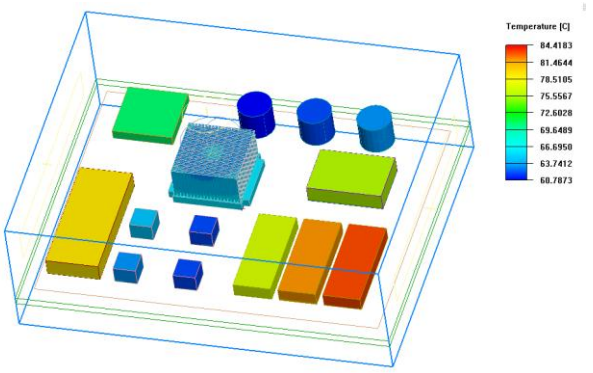


Fig. 4. Temperature distributions of the whole cabinet.

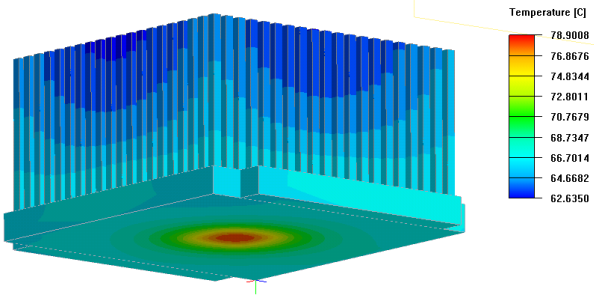


Fig. 5. Temperature distributions on the aluminum heat sink.

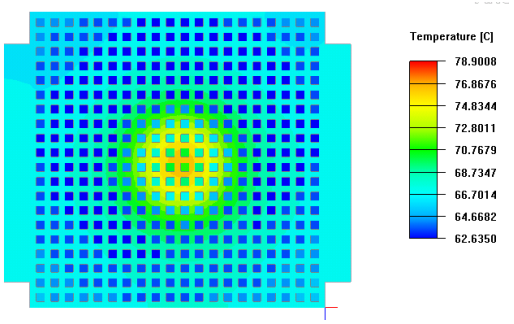


Fig. 6. Temperature distributions on the pins and base plate of the heat sink.

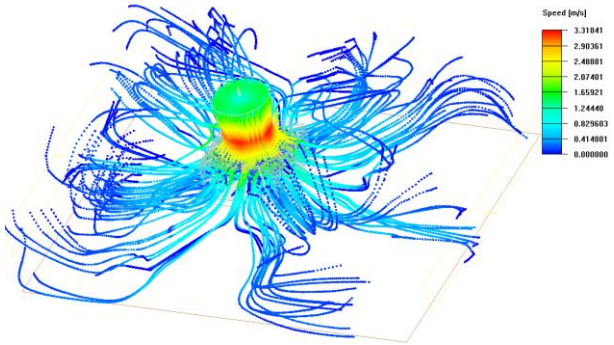


Fig. 7. Path lines and velocity vectors for the heat sink.

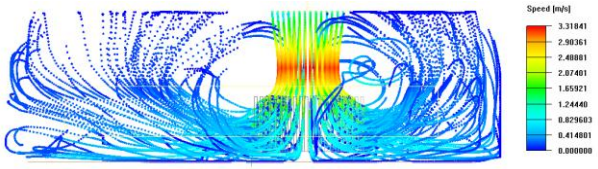


Fig. 8. Path lines and velocity vectors in the x-y view.

Velocity vectors distribution of the air inside the cabinet is obtained from the results as shown in Fig. 7. Maximum velocity of 3.3 m/s is recorded in the *y* axis at the fan entrance and decreases to a minimum value of 0.01m/s at the side surfaces of the cabinet near the outlet grilles. To clearly show the air passing through the pins of the heat sink, air flow pattern in the *x-y* plane is depicted in Fig. 8.

### *B. Effect of Heat Sink Materials*

We consider improving the thermal conductivity by using copper instead of aluminum. First, the four fins at the center of the heat sink are modified to be copper, but the thermal performance of the heat sink is not affected, indicating that these fins do not contribute much to the heat transfer. This result is consistent with the previous analyses where removing the four center fins did not change the temperature distribution [10]. However, when all of the fins are made out of copper, the maximum temperature on the heat sink decreases by 6.4 °C, as shown in Fig. 9. It is also observed from Fig. 9 that the minimum temperature increases by more than 1 °C. Therefore, the temperature gradients on the heat sink are observed to be smaller due to the high thermal conductivity of copper. The difference between the maximum and the minimum temperatures on the copper heat sink is less than 9 °C, whereas for the aluminum heat sink it is around 16 °C.



ISSN: 2278 – 7798 

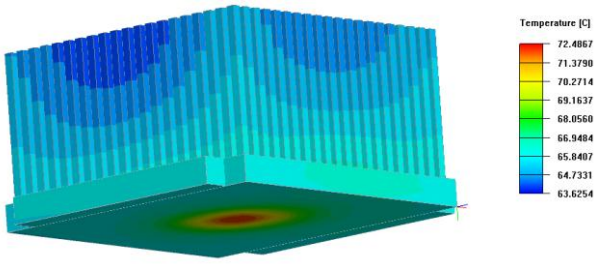


Fig. 9. Temperature distributions on the copper heat sink.

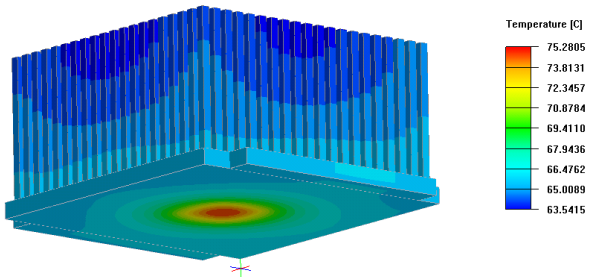


Fig. 10. Temperature distributions on the heat sink with thin base.

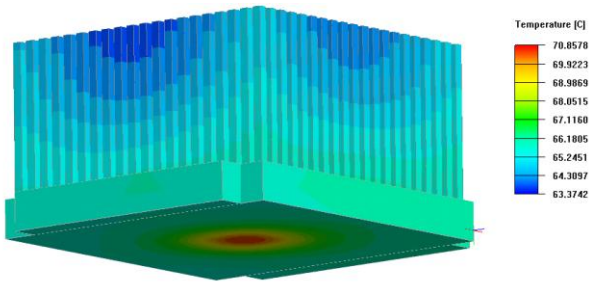


Fig. 11. Temperature distributions on the heat sink with thick base.

### *C. Effect of Base Thicknesses*

In order to investigate the base thickness effect, we calculate two cases based on the copper heat sink, in which the base thickness is normally 9 mm. In this part, the thickness is increased and decreased by 3 mm while keeping the fin lengths constant. Figures 10 and 11 show the temperature distributions on the thin and thick cases, respectively. It is seen that the maximum temperature on the heat sink increases by 2.8 °C for thin case while decreases by 1.6 °C for thick case. In order to clearly show the effect of base thicknesses, the temperature distributions on the line through the center of the heat sink are compared in Fig. 12. It is seen that the heat sink with the thinner base has higher temperatures. The tip temperatures are also very high since the temperature gradient on the fin along the fin length is small. As seen from Fig. 12, the thinner base results are not acceptable, the cooling effect is worse than the aluminum heat sink and longer fins should be used in order to decrease the maximum temperature on the heat sink. For the heat sinks whose base width is larger than the footprint of the heat source, which is the case here, the in-plane conduction resistance should be considered. Therefore, higher base thicknesses decrease the in-plane resistance as observed from Fig. 12. On the other hand, if the heat source and heat sink have the same width, it is better to make the base thinner to decrease the conduction resistance from the base to the fin tip direction.

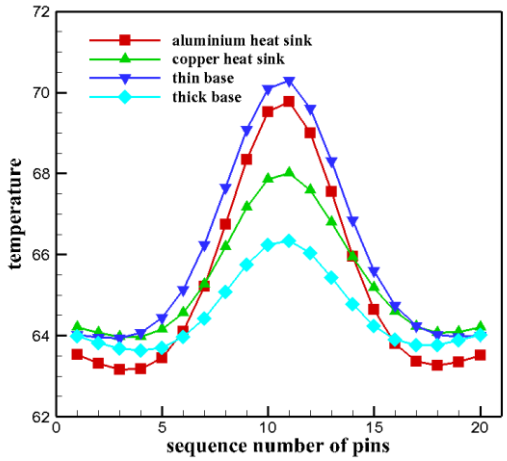


Fig. 12. Temperature plots on the base reference line for heat sinks with different materials and base thicknesses.

## [5] CONCLUSION

In this paper, the flow and temperature fields of an airtight cabinet are investigated using the the CFD software Icepak. The analysis shows that the cabinet having a 80 W power device can be satisfactorily cooled by the forced convection air cooling.

The effects of fin materials and base plate thicknesses on the thermal performance of the heat sink were studied. In the current study, it was seen that when the fin material is selected to be copper rather than aluminum, the thermal resistance of the heat sink decreases as expected. However, this makes the heat sink more expensive and heavier. The heat sink base thickness is also a parameter for improvement. When the base plate thickness was increased, the heat sink performed better. However, there are space limitations for every heat sink in a cabinet. Therefore, the total height of the heat sink should be considered together with the space limitations when increasing the height of the heat sink.

From this study it was found that CFD analysis can improve the thermal design by reducing the experimental cost, time and energy. Using CFD simulations, it is possible to come up with a new heat sink design which has better thermal performance and uses less material. The CFD analysis has become a powerful numerical tool which is widely used to get the thermal distributions in the electronic equipment. This paper would induce more engineers to explore the studies on application of CFD in electronics industries.

## REFERENCES

[1] R. L. Webb, "Next generation devices for electronic cooling with heat rejection to air," *Trans. ASME, J. Heat Transfer*, vol. 127, pp. 2–10, 2005.
[2] C. W. Yu and R. L. Webb, "Thermal design of a desktop computer system using CFD analysis," in *Proc. 17th IEEE Semi-Therm Symp*., 2001, pp. 18–26.
[3] R. Biswas, R. B. Agarwal, A. Goswami, and V. Mansingh, "Evaluation of airflow prediction methods in compact electronic enclosures," in *Proc. 15th IEEE Semi-Therm Symp*., 1999, pp. 48–53.
[4] R. L. Linton and D. Agonefer, "Coarse and detailed CFD modelling of a finned heat sink," *IEEE Trans. Compon., Packag., Manuf. Technol.- Part A*, vol. 18, no. 3, pp. 517–520, Sep. 1995.
[5] P. Sathyamurthy, P. W. Runstadler, and S. Lee, "Numerical and experimental evaluation of planar and staggered heat sinks," in *Proc. IEEE Inter Soc. Conf. Thermal Phenomena*, 1996, pp. 132–139.



ISSN: 2278 – 7798 

[6] X. Yu, J. Feng, Q. Feng, and Q.Wang, "Development of a plate-pin fin heat sink and its performance comparisons with a plate fin heat sink," *Appl. Thermal Eng*., vol. 25, pp. 173–182, 2005.
[7] V. Eveloy, P. Rodgers, and M. S. J. Hashmi, "Numerical prediction of electronic component heat transfer: An industry perspective," in *Proc. 19th IEEE Semi-Therm Symp*., 2003, pp. 14–26.
[8] N. Afgan, M. G. Carvalho, S. Prstic, and A. Bar-Cohen, "Sustainability assessment of aluminum heat sink design," *Heat Transfer Eng*., vol. 24, pp. 39–48, 2003.
[9] A. Bar Cohen, R. Bahadur, and M. Iyengar, "Least-energy optimization of air-cooled heat sinks for sustainability-theory, geometry and material selection," *Energy*, vol. 31, pp. 579–619, 2006.
[10] E. Öztürk, "CFD analyses of heat sinks for CPU cooling with Fluent," M.S. thesis, Dept. Mech. Eng., Middle East Tech. Univ, Ankara, Turkey, 2004.

**Heng Ren** received B. E. degree in Engineering Mechanics from Lanzhou University and Ph. D degree in Engineering Mechanics from University of Science and Technology of China. Presently working as an engineer in China Electronics Technology Group Corporation No.38 Research Institute. His research areas are electronic equipment thermal control and computational fluid dynamics.



ISSN: 2278 – 7798 